




## Article

# Synthesis of Methyldopa–Tin Complexes and Their Applicability as Photostabilizers for the Protection of Polyvinyl Chloride against Photolysis

Noor Naoom <sup>1</sup>, Emad Yousif <sup>1</sup> , Dina S. Ahmed <sup>2</sup>, Benson M. Kariuki <sup>3</sup>  and Gamal A. El-Hiti <sup>4,\*</sup> <sup>1</sup> Department of Chemistry, College of Science, Al-Nahrain University, Baghdad 64021, Iraq<sup>2</sup> Department of Medical Instrumentation Engineering, Al-Mansour University College, Baghdad 64201, Iraq<sup>3</sup> School of Chemistry, Cardiff University, Main Building, Park Place, Cardiff CF10 3AT, UK<sup>4</sup> Department of Optometry, College of Applied Medical Sciences, King Saud University, Riyadh 11433, Saudi Arabia

\* Correspondence: gelhiti@ksu.edu.sa; Tel.: +966-1-1469-3778; Fax: +966-1-1469-3536

**Abstract:** Polyvinyl chloride (PVC) is a ubiquitous thermoplastic that is produced on an enormous industrial scale to meet growing global demand. PVC has many favorable properties and is used in various applications. However, photodecomposition occurs when harsh conditions, such as high temperatures in the presence of oxygen and moisture, are encountered. Thus, PVC is blended with additives to increase its resistance to deterioration caused by exposure to ultraviolet light. In the current research, five methyldopa–tin complexes were synthesized and characterized. The methyldopa–tin complexes were mixed with PVC at a concentration of 0.5% by weight, and thin films were produced. The capability of the complexes to protect PVC from irradiation was shown by a reduction in the formation of small residues containing alcohols, ketones, and alkenes, as well as in weight loss and in the molecular weight of irradiated polymeric blends. In addition, the use of the new additives significantly reduced the roughness factor of the irradiated films. The additives containing aromatic substituents (phenyl rings) were more effective compared to those comprising aliphatic substituents (butyl and methyl groups). Methyldopa–tin complexes have the ability to absorb radiation, coordinate with polymeric chains, and act as radical, peroxide, and hydrogen chloride scavengers.

**Keywords:** methyldopa–tin complexes; photolysis; polyvinyl chloride; weight loss; molecular weight depression; surface morphology



**Citation:** Naoom, N.; Yousif, E.; Ahmed, D.S.; Kariuki, B.M.; El-Hiti, G.A. Synthesis of Methyldopa–Tin Complexes and Their Applicability as Photostabilizers for the Protection of Polyvinyl Chloride against Photolysis. *Polymers* **2022**, *14*, 4590. <https://doi.org/10.3390/polym14214590>

Academic Editors: Olga Klinkova, Alex A. Volinsky, Alexander Kondratov and Ekaterina Marchenko

Received: 26 September 2022

Accepted: 27 October 2022

Published: 28 October 2022

**Publisher's Note:** MDPI stays neutral with regard to jurisdictional claims in published maps and institutional affiliations.



**Copyright:** © 2022 by the authors. Licensee MDPI, Basel, Switzerland. This article is an open access article distributed under the terms and conditions of the Creative Commons Attribution (CC BY) license (<https://creativecommons.org/licenses/by/4.0/>).

## 1. Introduction

The demand for plastics is projected to keep increasing due to their versatile properties [1]. Plastics are strong, light, and inexpensive and can be produced in different forms to suit specific applications [2–4]. Plastics are, therefore, efficient replacements for some common construction materials, such as steel, wood, and glass. However, a drawback is that plastics suffer from photodegradation when exposed to ultraviolet (UV) light at high temperatures in environments rich in oxygen [5]. Photodegradation leads to deterioration in their mechanical and physical properties resulting in color changes, deformation, and the appearance of cracks [6]. It is, therefore, necessary to enhance the long-term resistance of plastics to photodegradation in hot and humid conditions during manufacturing [7].

Polyvinyl chloride (PVC) is a thermoplastic polymer that ranks in the top three, along with polyethylene and polypropylene, in terms of commercial production [8,9]. PVC is inexpensive, possesses excellent mechanical properties, is available in different forms, and is simple to process and shape. It has many industrial applications, including water piping, insulation, flooring, roofing, packaging, medical instruments, cars, and furniture [10,11]. The downside, however, is that PVC waste is hazardous to humans,

animals, and the environment. Furthermore, the photodecomposition of the material can occur in the presence of oxygen at high temperatures if PVC is exposed to light in humid conditions [12,13]. Two strategies are, therefore, employed to reduce PVC waste generation and its photodecomposition. The first strategy involves recycling and reusing PVC waste. Various effective processes have been employed for the recycling of PVC [14–16]. The second strategy involves the addition of stabilizers to suppress the photodecomposition, which can lead to the deterioration of properties and shortening of the duration of useful life for PVC [17]. PVC photodegradation is autocatalytic and leads to the production of chains that contain conjugated double bonds as a result of dehydrochlorination and the formation of volatile products. In addition, it causes a decrease in the molecular weight, a reduction in weight, and discoloration of PVC. The main reasons for PVC photodegradation are chain scissions and cross-linking due to the elimination of hydrogen chloride (HCl) [18–22].

Recent research has focused on synthesizing new organic PVC stabilizers with high aromaticity and heteroatom concentrations [5]. These additives act to protect polymeric materials from harmful irradiation and reduce the changes in mechanical properties, cracking, and discoloration [23,24]. Photostabilizers absorb energy from irradiation and quench active and volatile species, such as radicals and HCl [25]. The additives should be non-volatile, nontoxic, and inexpensive and used at low concentrations to avoid changes in the color of PVC [26]. Many potentially commercial PVC stabilizers are banned mainly because of associated hazards or the requirement for co-stabilizers [27–30]. Alternatives such as Schiff bases, polyphosphates, and complexes containing tin and aromatic moieties were synthesized, and their role as PVC additives has been assessed [31–35].

Tin complexes containing organic residues are highly stable and have various medicinal applications [36–40]. Additionally, tin complexes are used in catalysis, wood preservatives, agrochemicals, disinfectants, biocides, and polymer additives [41]. Methyl dopa is an antihypertensive medication and can be used to lower blood pressure [42]. It is inexpensive, commercially available, stable, nontoxic, and contains an aromatic moiety and heteroatoms (36.9% by weight). Therefore, methyl dopa is a good candidate for inclusion in the additives used to protect PVC from photolysis. We report the synthesis of new methyl dopa–tin complexes and investigate their effect on PVC photodecomposition.

## 2. Materials and Methods

### 2.1. Materials and Samples Preparation

Merck (Gillingham, UK) supplied tin chlorides (95–98%), methyl dopa (99%), and solvents (analytical grades), which were used as received. The PVC ( $M_v = \text{ca. } 180,000$ ) was purchased from Petkim Petrokimya (Istanbul, Turkey). The PVC blends were prepared in a Kerry PUL 55 ultrasonic bath (Kerry Ultrasonics Ltd., Hitchin, UK). An accelerated weather meter QUV tester (Homestead, FL, USA) was used for the irradiation ( $365 \text{ nm}$ ;  $6.2 \times 10^{-9} \text{ Einstein dm}^{-3} \text{ s}^{-1}$ ) of the films at room temperature. The tester is equipped with two identical 40 watts fluorescent lamps (UV-B 365), one on each side. The distance between the films and the tester was kept at 10 cm. The PVC materials were rotated occasionally in order for the films to be irradiated equally from all sides.

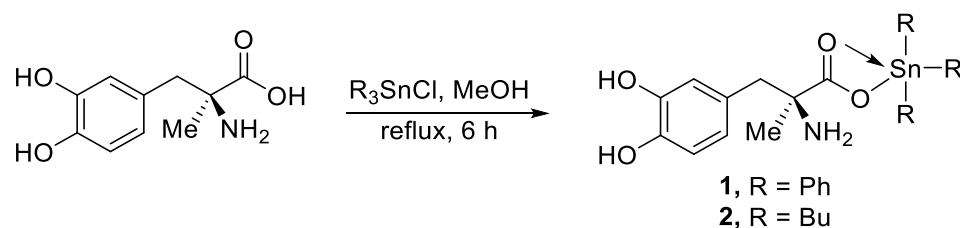
### 2.2. Methods

The microanalytical analysis was performed using a Shimadzu AA-6880 spectrophotometer (Tokyo, Japan). A Shimadzu FT-IR8400S (Tokyo, Japan) was used to record the infrared (IR) spectra ( $400\text{--}4000 \text{ cm}^{-1}$ ). The nuclear magnetic resonance (NMR) spectra were recorded in deuterated dimethyl sulfoxide ( $\text{DMSO-d}_6$ ) using a Bruker Advance DRX 400 MHz spectrometer (Zürich, Switzerland). An Ostwald U-Tube Viscometer (Ambala, India) was used to measure the viscosity of solutions. A Bruker XFlash 6-10 (Tokyo, Japan) was used to record energy-dispersive X-ray (EDX) spectra. Before the EDX spectra were recorded, the films were coated with a thin layer (ca. 15 nm) of gold (Au). The optical images were recorded using a Meiji Techno microscope (Tokyo, Japan). The atomic force microscopy (AFM) images were captured on a Veeco instrument (Plainview, NY, USA). The

scanning electron microscopy (SEM) images were recorded using an Inspect S50 microscope (FEI Company, Czechia, Czech Republic; 15 kV).

### 2.3. Synthesis of 1 and 2

A mixture of methyl dopa (0.21 g, 1 mmol) and  $\text{Ph}_3\text{SnCl}$  (0.39 g, 1 mmol) or  $\text{Bu}_3\text{SnCl}$  (0.33 g, 1 mmol) in MeOH (30 mL) was refluxed for 6 h (Scheme 1). The white solid obtained was filtered, washed with MeOH, and dried in a vacuum oven at 45 °C for 6 h to give 1 or 2 in a high yield (Table 1).



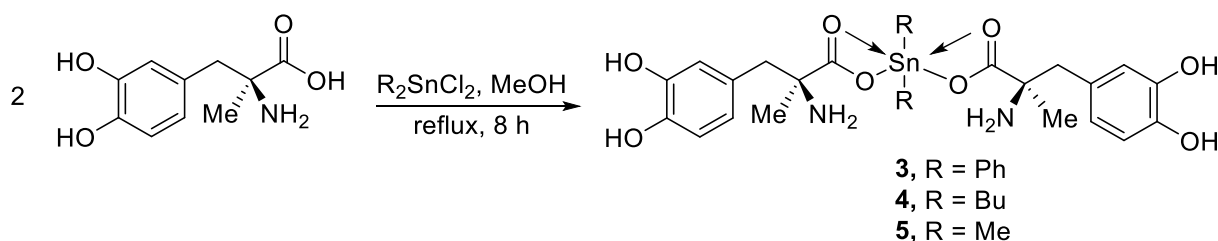
**Scheme 1.** Synthesis of 1 and 2.

**Table 1.** Some physical data for 1–5.

Complex	Melting Point (°C)	Yield (%)	Calculated (Found; %)			
			C	H	N	Sn
1	105–107	83	60.03 (60.07)	4.86 (4.89)	2.50 (2.52)	21.19 (21.23)
2	174–176	74	52.82 (52.86)	7.86 (7.92)	2.80 (2.84)	23.73 (23.76)
3	123–125	84	55.43 (55.46)	9.94 (9.97)	4.04 (4.06)	17.12 (17.14)
4	108–110	81	51.47 (51.49)	6.48 (6.51)	4.29 (4.33)	18.17 (18.20)
5	178–180	78	46.42 (46.47)	5.31 (5.35)	4.92 (4.93)	20.86 (20.91)

### 2.4. Synthesis of 3–5

A mixture of methyl dopa (0.42 g, 2 mmol) and  $\text{Ph}_2\text{SnCl}_2$  (0.34 g, 1 mmol),  $\text{Bu}_2\text{SnCl}_2$  (0.30 g, 1 mmol), or  $\text{Me}_2\text{SnCl}_2$  (0.22 g, 1 mmol) in MeOH (30 mL) was refluxed for 8 h (Scheme 2). The resulting white solid was filtered, washed with MeOH, and dried in a vacuum oven at 45 °C for 6 h to produce 3, 4, or 5 in a high yield (Table 1).



**Scheme 2.** Synthesis of 3–5.

### 2.5. Preparation of PVC Films

Tetrahydrofuran (THF; 100 mL) was added to a mixture of the appropriate complex (25 mg) and PVC (5.0 g). The mixture was stirred for 2 h at 25 °C to ensure the formation of a homogenous blend. The solution was poured into a glass plate containing holes (thickness = 40 μm). The plate was left in the air at 25 °C for 24 h to dry. A vacuum oven (40 °C; 8 h) was used to ensure the dryness of the films.

### 2.6. Assessment of IR Spectra

The PVC photodecomposition process generates active species (e.g., free radicals), which initiates the elimination of volatiles and bond cleavage [43]. As a result, fragments

containing hydroxyl (OH; e.g., alcohols), carbonyl (C=O; e.g., ketones), and carbon–carbon double bonds (C=C; e.g., alkenes) are produced [44,45]. The IR absorption bands corresponding to the OH, C=O, and C=C groups appear at about 3497, 1714, and 1612  $\text{cm}^{-1}$ , respectively. The intensities of the peaks corresponding to these functional groups can be monitored using IR spectroscopy during irradiation. A standard peak that appeared at 1328  $\text{cm}^{-1}$  (C–H bond) was chosen for comparison [46]. Equation (1) was used to calculate the indices ( $I_s$ ) of the hydroxyl, carbonyl, and polyene groups ( $I_{\text{OH}}$ ,  $I_{\text{C=O}}$ , and  $I_{\text{C=C}}$ , respectively) as a function of the absorbances of the functional groups ( $A_s$ ) and the standard peak ( $A_r$ ).

$$I_s = \frac{A_s}{A_r} \quad (1)$$

### 2.7. Assessment of Weight Loss

PVC irradiation causes weight loss due to the formation of small fragments. Equation (2) can be used to calculate the percentage of PVC weight loss at a time ( $t$ ) of irradiation [47]. The weight loss was calculated using the weights of the non-irradiated and irradiated PVC films ( $W_0$  and  $W_t$ , respectively) [47].

$$\text{Weight loss (\%)} = \frac{W_0 - W_t}{W_0} \times 100 \quad (2)$$

### 2.8. Assessment of Average Molecular Weight ( $M_v$ )

PVC irradiation decreases the  $M_v$  as a result of the elimination of small residues, including volatiles. Following irradiation, the blends were dissolved in a solvent (THF), and their intrinsic viscosities  $[\eta]$  were measured. Filtration was necessary to remove any insoluble polymeric residues as a result of cross-linking of PVC. The decreases in  $M_v$  are directly proportional to the  $[\eta]$ . The Mark–Houwink relationship (Equation (3)) was used to calculate the  $M_v$  of the irradiated blends [48]. The viscosity of the PVC films was determined in THF at 25 °C.

$$[\eta] = 1.38 \times 10^{-4} M_v^{0.77} \quad (3)$$

## 3. Results and Discussion

### 3.1. Synthesis of Complexes 1–5

The reaction of methyl dopa and trisubstituted tin chlorides in a 1:1 molar proportion gave complexes **1** and **2** (Scheme 1) 83% and 74% yields, respectively (Table 1). The reaction of methyl dopa with disubstituted tin dichlorides in a 2:1 molar proportion gave complexes **3–5** (Scheme 2) in 78–84% yields (Table 1). The procedures were simple, effective, general, repeatable, and high yielding. In addition, the introduction of substituents (aliphatic and aromatic) in different numbers (di and tri) to the skeleton of the complexes was achievable.

The IR spectra of methyl dopa–tin complexes **1–5** showed several absorption bands corresponding to the OH (3217–3279  $\text{cm}^{-1}$ ), Sn–C (511–530  $\text{cm}^{-1}$ ), and Sn–O (443–457  $\text{cm}^{-1}$ ) bonds (Table 2). The presence of two absorption bands (symmetric and anti-symmetric) for the  $\text{NH}_2$  (3473–3409  $\text{cm}^{-1}$ ) was observed in most cases (Table 2). The vibration signal of the asymmetric carbonyl group has shifted to a higher frequency due to coordination between the tin atom and the carboxylate group ( $\text{COO}^-$ ) oxygen. The difference ( $\Delta\nu$ ) between the asymmetric (asym) and symmetric (sym) vibration frequencies of the  $\text{COO}^-$  group was calculated to be between 237 and 285  $\text{cm}^{-1}$ . A value of  $\Delta\nu$  in this range indicates an intermediate state between monodentate and bidentate (anisobidentate) asymmetry [49,50].

**Table 2.** Selected FTIR spectral data for 1–5.

Complex	NH <sub>2</sub>	OH	C=O Asym	C=O Sym	$\Delta\nu$ (Asym—Sym)	Sn—C	Sn—O
1	3450, 3415	3271	1757	1487	270	511	443
2	3473, 3409	3217	1776	1491	285	530	455
3	3452, 3427	3277	1734	1491	243	522	443
4	3444, 3427	3252	1732	1493	239	524	443
5	3431	3279	1734	1497	237	514	457

The <sup>1</sup>H NMR spectra confirmed the presence of protons from both methyl dopa and substituted tin chloride (Table 3). It was noted that the peaks corresponding to the OH and NH<sub>2</sub> protons were broad, possibly due to the partial proton exchange with the deuterated solvent (DMSO-d<sub>6</sub>).

**Table 3.** <sup>1</sup>H NMR spectral data of 1–5.

Complex	<sup>1</sup> H NMR (400 MHz)
1	8.91 (br s, 1H, OH), 8.79 (br s, 1H, OH), 7.92–7.66 (m, 15H, 3 Ph), 6.60 (s, 1H, Ar), 6.52 (d, <i>J</i> = 7 Hz, 1H, Ar), 6.29 (d, <i>J</i> = 7 Hz, 1H, Ar), 3.45 (br s, 2H, NH <sub>2</sub> ), 2.90 (d, <i>J</i> = 14 Hz, 1H, 1H of CH <sub>2</sub> ), 2.65 (d, <i>J</i> = 14 Hz, 1H, 1H of CH <sub>2</sub> ), 1.28 (s, 3H, Me)
2	9.01 (br s, 1H, OH), 7.68 (br s, 1H, OH), 6.67 (d, <i>J</i> = 8 Hz, 1H, Ar), 6.64 (s, 1H, Ar), 6.51 (d, <i>J</i> = 8 Hz, 1H, Ar), 3.81 (br s, 2H, NH <sub>2</sub> ), 2.92 (d, <i>J</i> = 13 Hz, 1H, 1H of CH <sub>2</sub> ), 2.71 (d, <i>J</i> = 13 Hz, 1H, 1H of CH <sub>2</sub> ), 1.64 (br s, 6H, 3 CH <sub>2</sub> ), 1.56–1.48 (m, 12H, 6 CH <sub>2</sub> ), 1.24 (s, 3H, Me), 0.85 (t, <i>J</i> = 7 Hz, 9H, 3 Me)
3	9.01 (br s, 2H, 2 OH), 8.90 (br s, 2H, 2 OH), 7.41–7.30 (m, 10H, 2 Ph), 6.68 (s, 2H, Ar), 6.62 (d, <i>J</i> = 8 Hz, 2H, Ar), 6.48 (d, <i>J</i> = 8 Hz, 2H, Ar), 3.73 (br s, 4H, 2 NH <sub>2</sub> ), 2.92 (d, <i>J</i> = 14 Hz, 2H, 1H of CH <sub>2</sub> ), 2.86 (d, <i>J</i> = 14 Hz, 2H, 1H of 2 CH <sub>2</sub> ), 1.23 (s, 6H, 2 Me)
4	8.99 (br s, 2H, 2 OH), 8.12 (br s, 2H, 2 OH), 6.68 (d, <i>J</i> = 8 Hz, 2H, Ar), 6.63 (s, 2H, Ar), 6.50 (d, <i>J</i> = 8 Hz, 2H, Ar), 3.65 (br s, 4H, 2 NH <sub>2</sub> ), 2.97 (d, <i>J</i> = 13 Hz, 2H, 1 H of 2 CH <sub>2</sub> ), 2.81 (d, <i>J</i> = 13 Hz, 2H, 1H of 2 CH <sub>2</sub> ), 1.66 (br s, 4H, 2 CH <sub>2</sub> ), 1.51–1.42 (m, 8H, 4 CH <sub>2</sub> ), 1.26 (s, 6H, 2 Me), 0.82 (t, <i>J</i> = 7 Hz, 6H, 2 Me)
5	88.88 (br s, 2H, 2 OH), 7.96 (br s, 2H, 2 OH), 6.65 (d, <i>J</i> = 8 Hz, 2H, Ar), 6.53 (s, 2H, Ar), 6.51 (d, <i>J</i> = 8 Hz, 2H, Ar), 3.74 (br s, 4H, 2 NH <sub>2</sub> ), 2.96 (d, <i>J</i> = 14 Hz, 2H, 1 H of 2 CH <sub>2</sub> ), 2.76 (d, <i>J</i> = 14 Hz, 2H, 1H of 2 CH <sub>2</sub> ), 1.40 (s, 6H, 2 Me), 0.51 (s, 6H, 2 Me)

The structures of 1–5 were established further by the <sup>13</sup>C NMR spectral data (Table 4). The carbon atoms of the carbonyl groups were detected at very low fields in the region of 172.9–174.2 ppm.

**Table 4.** <sup>13</sup>C NMR spectral data of 1–5.

Complex	<sup>13</sup> C NMR (100 MHz)
1	173.1, 145.4, 144.9, 136.7, 128.9, 128.8, 128.4, 125.6, 121.6, 118.6, 116.0, 60.7, 42.5, 23.1
2	173.5, 145.5, 145.0, 126.3, 121.7, 118.6, 116.1, 60.9, 42.6, 28.6, 27.0, 23.1, 20.9, 14.3
3	172.9, 145.6, 145.3, 136.9, 128.8, 128.7, 128.2, 124.8, 121.6, 118.2, 116.1, 60.2, 42.3, 22.3
4	173.0, 145.5, 145.2, 125.0, 121.6, 118.3, 116.1, 60.3, 42.3, 28.0, 26.1, 22.5, 22.2, 14.2
5	174.2, 145.5, 145.1, 125.5, 121.7, 118.5, 116.0, 60.6, 42.4, 23.0, 6.1

### 3.2. The EDX Spectroscopy of PVC Films

Homogenous, colorless thin films were produced by mixing the appropriate methyl dopa-tin complex (0.5% by weight) with PVC. EDX spectroscopy was used to evaluate the elemental composition of the PVC blends [51–53]. The EDX spectra of the non-irradiated films exhibited highly abundant absorption bands corresponding to the Cl atoms of PVC,

as well as those for N and O from methyl dopa and Sn, but in lower proportions (Figure 1). The peak assignment agrees with those previously reported for PVC blends with other additives containing tin and related elements [31].

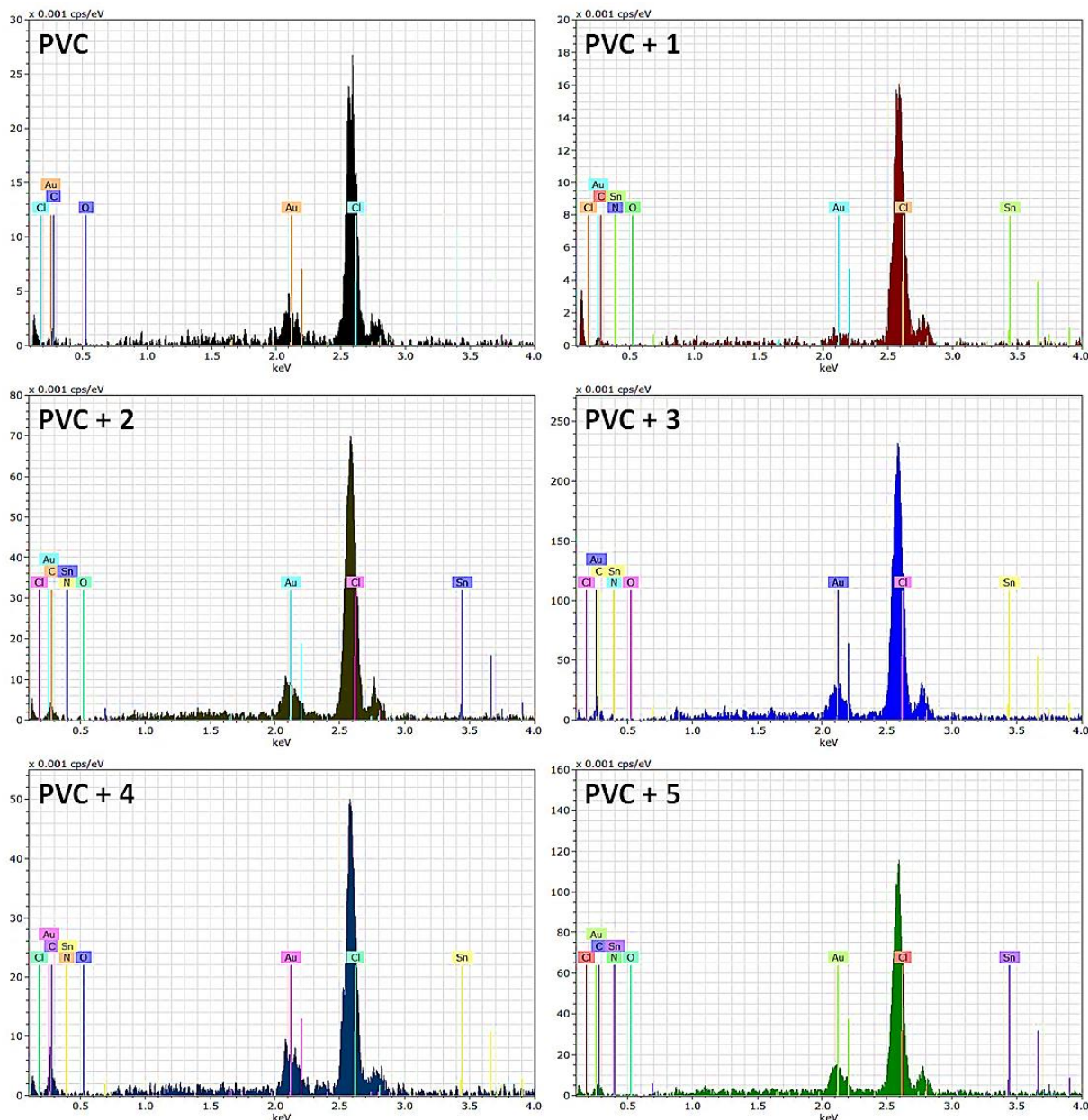


**Figure 1.** EDX spectra of PVC films.

The analysis of the EDX mapping indicated that metal complexes were completely dispersed and compatible with the polymeric matrix. The elements from metal complexes (Sn, N, and O) were distributed homogeneously in a similar percentage. Following irradiation, the chlorine content dropped due to the elimination of volatiles, including HCl. The blends containing methyl dopa–tin complex showed a lesser decrease in the chlorine content compared to the blank film. Clearly, additives 1–5 can be used to reduce PVC photodecomposition. The irradiated PVC film containing complex 1 shows the highest chlorine content.

It was noted that the color of the PVC films became darker as the irradiation time increased (Figure 2).

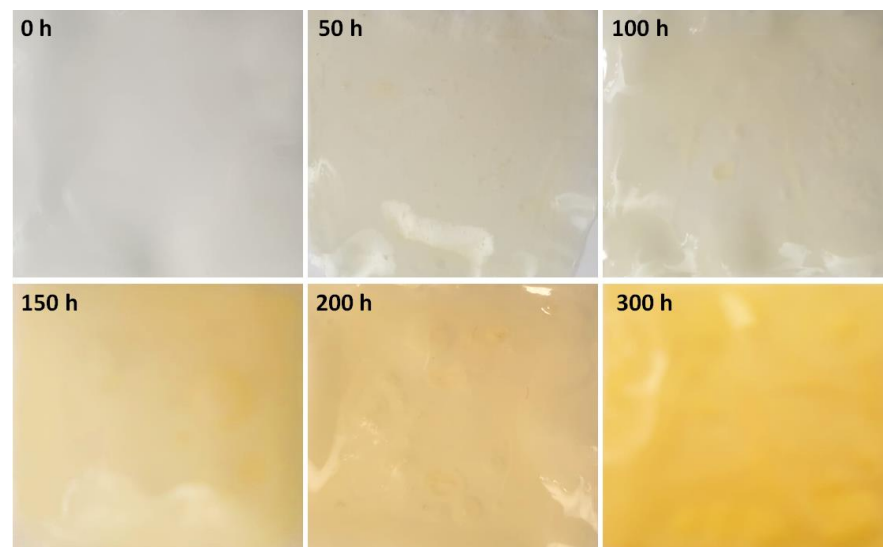


**Figure 2.** Color of PVC films after different irradiation times.

### 3.3. IR Spectral Study of PVC Films

Photooxidation of PVC causes the degradation of polymeric chains and produces fragments containing alcohols (OH), ketones (C=O), and polyenes (C=C) [54,55]. The IR spectra of the PVC films were recorded at intervals of 50 h during irradiation. The intensity of the absorption peaks corresponding to the OH ( $3497\text{ cm}^{-1}$ ), C=O ( $1714\text{ cm}^{-1}$ ), and C=C ( $1612\text{ cm}^{-1}$ ) increased due to irradiation (Figure 3). Therefore, the intensities of these peaks were monitored over time and compared to the C–H bond ( $1328\text{ cm}^{-1}$ ), which act as a reference. Irradiation has little effect on the intensity of the C–H bonds since they are highly stable.

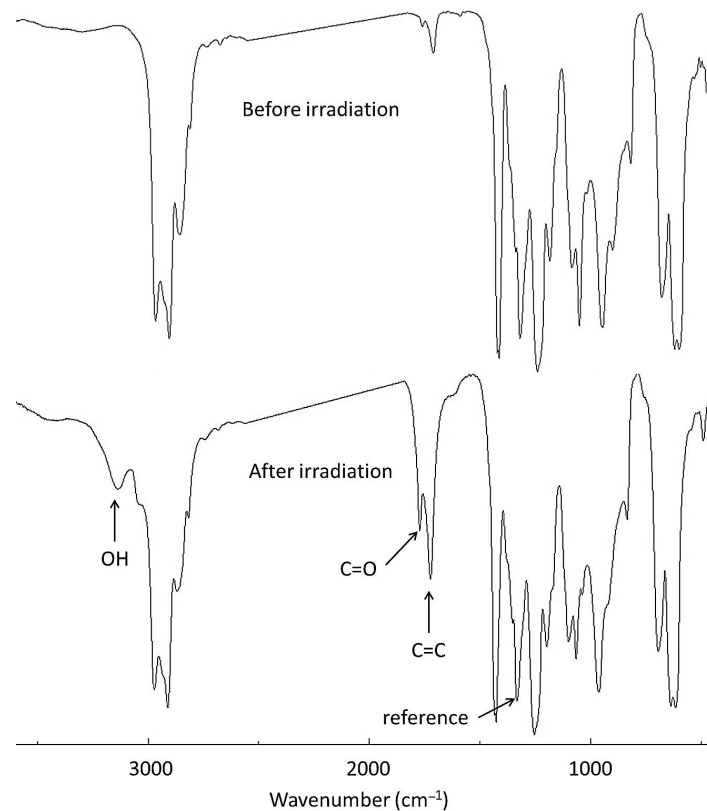


**Figure 3.** FTIR spectrum of PVC film before and after irradiation (300 h).

The indices of the OH ( $I_{OH}$ ), C=O ( $I_{C=O}$ ), and C=C ( $I_{C=C}$ ) groups of the irradiated films were calculated using Equation (1) and presented graphically in Figures 4–6, respectively. The  $I_{OH}$ ,  $I_{C=O}$ , and  $I_{C=C}$  increased significantly as the irradiation process progressed. The increases were very sharp at the beginning of the irradiation and then continued to increase steadily. The films containing 1–5 showed lower increases in the indices of functional groups compared to pure PVC film. It was clear that methyldopa–tin complexes act as photostabilizers to protect PVC. The additives with the highest aromaticity content (i.e., 1 and 3) showed the greatest stabilizing effect. The complexes were stabilized in the following order: triphenyl (1), diphenyl (3), tributyl (2), dibutyl (4), and dimethyl (5). The complexes interact with the active species (e.g., radicals), causing PVC photodegradation and the formation of active intermediates. The stability of the intermediates is highly dependent on the number and type of aromatic moieties present. Aromatic rings tend to reduce the energy of intermediates through resonance. At the end of the irradiation process, the  $I_{OH}$  were 0.44 (blank PVC film), 0.21 (PVC + 1), 0.29 (PVC + 2), 0.26 (PVC + 3), 0.32 (PVC + 4), and 0.35 (PVC + 5). Similar trends were observed for the  $I_{C=O}$  and  $I_{C=C}$  values.

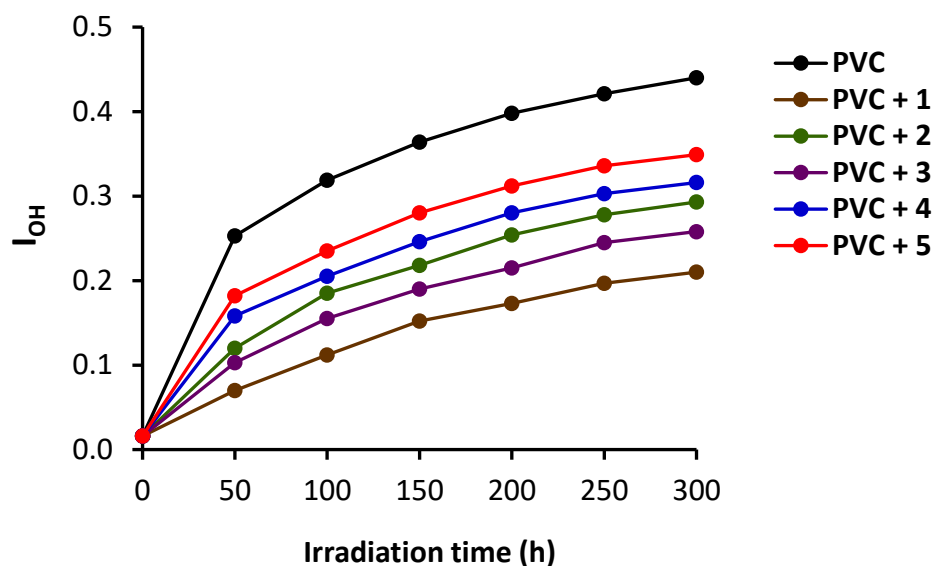


Figure 4. The  $I_{OH}$  of the irradiated PVC films.

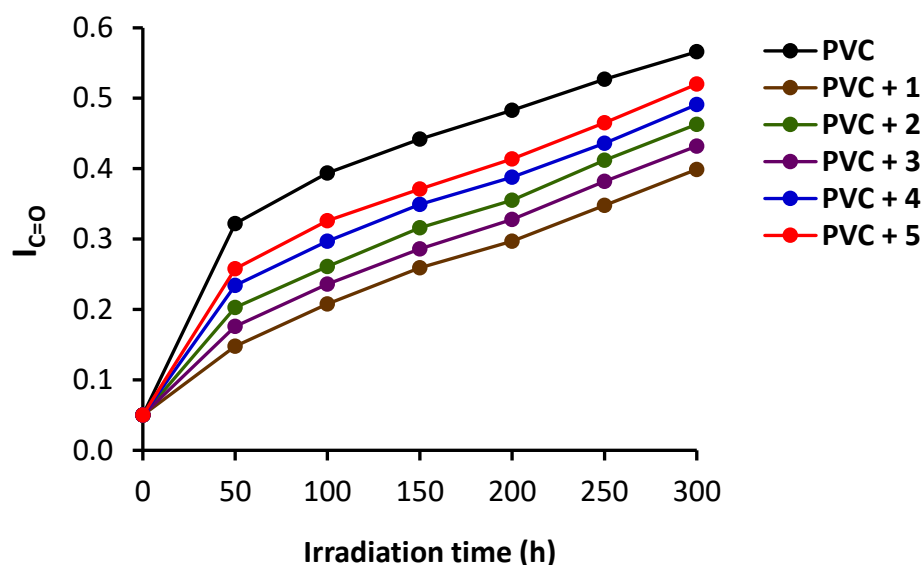


Figure 5. The  $I_{C=O}$  of the irradiated PVC films.



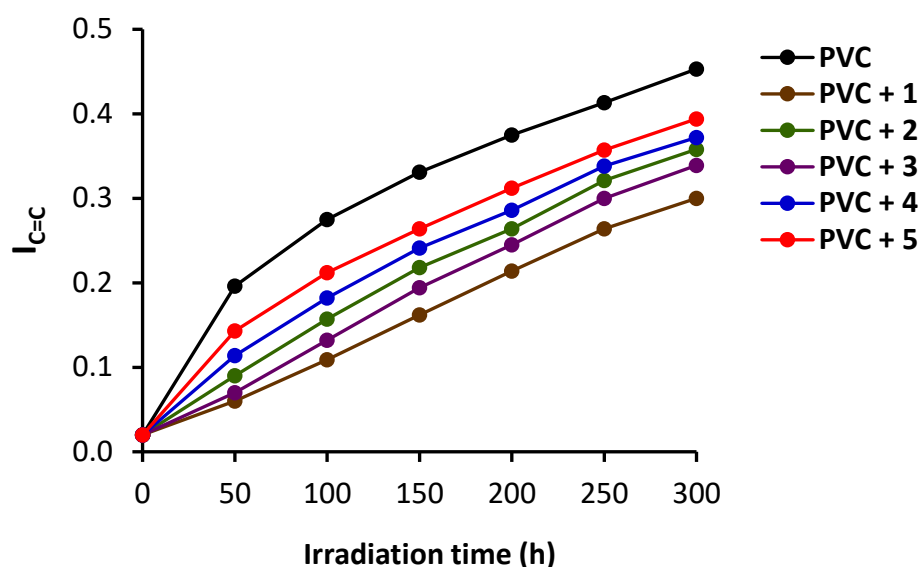


Figure 6. The  $I_{C=C}$  of the irradiated PVC films.

### 3.4. Weight Loss Investigation of PVC Films

Photodegradation of PVC leads to the elimination of volatiles and causes a reduction in weight [56]. The weight loss percentages of the PVC films due to irradiation were calculated using Equation (2) and are presented graphically in Figure 7. Generally, weight loss increases as radiation time progresses, and it was sharpest in the first 100 h. The greatest weight loss was seen for the pure PVC film, and the use of methyl dopa–tin complexes as photostabilizers led to a significant reduction in weight loss in comparison. At the end of irradiation, the weight loss (%) was 1.45% (blank PVC film), 0.53% (PVC + 1), 0.86% (PVC + 2), 0.66% (PVC + 3), 0.96% (PVC + 4), and 1.10% (PVC + 5). Again, highly aromatic complexes (i.e., 1 and 3) led to the highest stabilizing effect compared to the others.

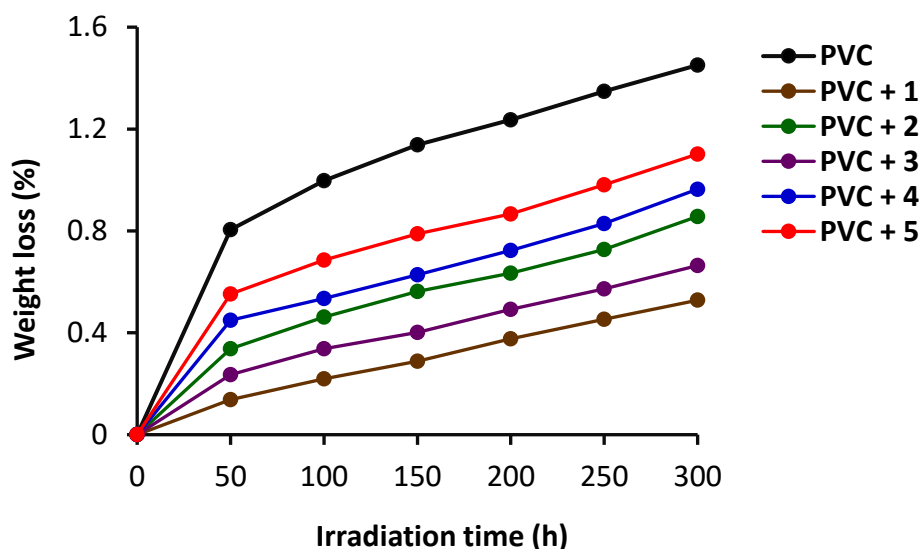
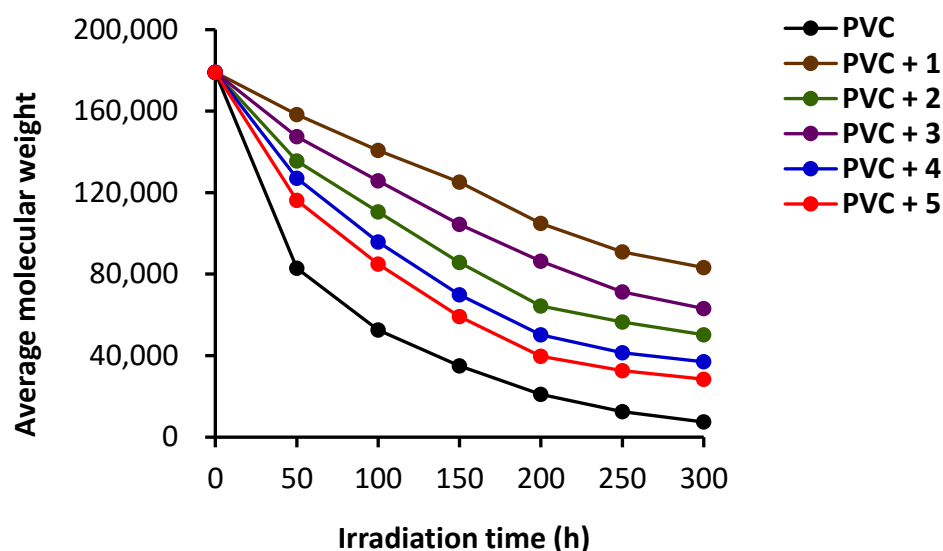


Figure 7. Weight loss (%) of the irradiated PVC films.

### 3.5. Viscosity Average Molecular Weight ( $M_v$ ) Study of PVC Films

Both chain scission and cross-linking are common processes resulting from PVC photodegradation [54,57]. These processes can lead to a reduction in  $M_v$  due to the elimination of small fragments. The  $M_v$  for the irradiated PVC was calculated using Equation (3) for different irradiation times and is presented graphically in Figure 8. The viscosity of solutions of PVC dropped as irradiation time increased. The drop in  $M_v$  is

generally massive and is initially particularly noticeable for pure PVC film. It was clear that the additives hindered the decrease in Mv. For pure PVC, the reduction in Mv was 54% after 50 h, 71% after 100 h, 88% after 200 h, and 96% after 300 h of irradiation. In contrast, the irradiated PVC film containing **1** led to a decrease in Mv by 12%, 21%, 41%, and 53% after 50, 100, 200, and 300 h of irradiation, respectively.



**Figure 8.** The Mv of the irradiated PVC films.

### 3.6. Surface Assessment of the Irradiated PVC Films

Various types of microscopy techniques, including optical, SEM, and AFM, have been utilized to assess the damage that occurs on the surface of irradiated PVC films [58–61]. These tools are good for monitoring the changes caused in the surface of polymers due to irradiation. In addition, the AFM provides clear non-distorted two- and three-dimensional images to provide a clear picture of the roughness factor of the irradiated surface. Generally, non-irradiated PVC films have a high degree of homogeneity, regularity, and smoothness [31]. Optical microscopy (Figure 9), SEM (Figure 10), and AFM (Figure 11) images revealed more damage (e.g., cracks, spots, darkness, irregularities, and roughness) on the surface of irradiated blank PVC in comparison to those containing 1–5. For example, the SEM images indicated the random distribution and incorporation of metal complexes within the PVC blend. The elimination of HCl and volatiles, bond cleavages, and chain scission are the main causes of surface damage. The results provided additional evidence for the efficacy of methyl dopa–tin complexes as PVC photostabilizers. The microscopic images of the surface of the irradiated PVC film containing complex **1** showed the least damage in terms of heterogeneity and roughness. Thus, for example, the roughness factor (Rq) for the irradiated films was 458.6 (blank PVC film), 28.3 (PVC + 1), 52.8 (PVC + 2), 40.2 (PVC + 3), 68.3 (PVC + 4), and 70.1 (PVC + 5). It was clear that complex **1** led to a reduction in Rq by 16.2-fold, which is remarkable.

The use of methyl dopa–tin complexes led to a significant improvement in the Rq and showed great efficiency in stabilizing PVC compared to many other PVC additives that have recently been reported [62–72]. For example, organotin complexes containing naproxen [62], carvedilol [63], furosemide [64], valsartan [65], telmisartan [66], trimethoprim [67], norfloxacin [68], and levofloxacin [69] led to a reduction in the Rq by 5.2–15.4 fold. On the other hand, organotin complexes with a high level of heteroatoms and aromaticity (e.g., ciprofloxacin, 4-(benzylideneamino)benzenesulfonamide, and 4-methoxybenzoic acid) resulted in greater improvement in the Rq (16.6–21.2 fold) [70–72].

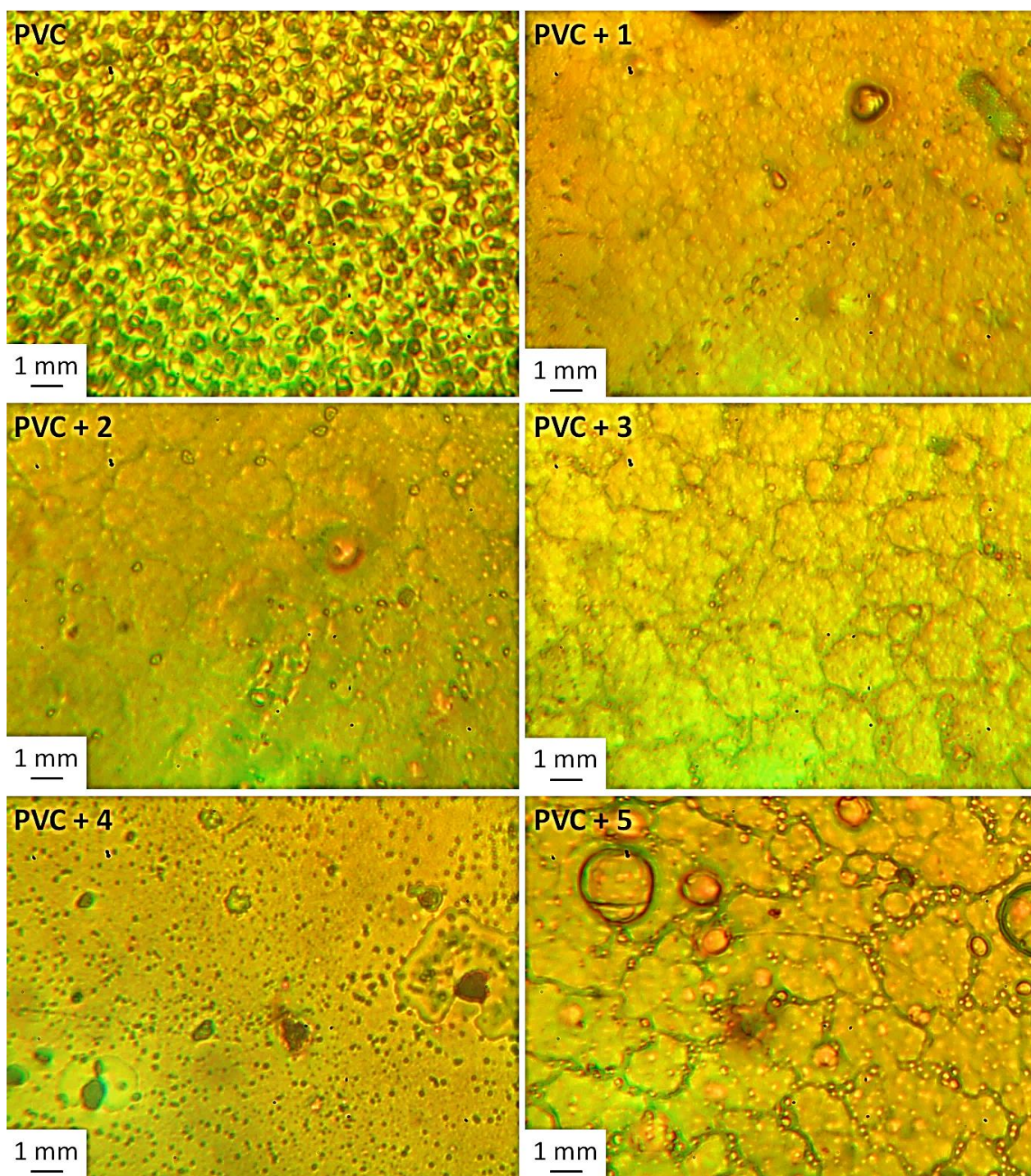


**Figure 9.** Images under the optical microscope for the irradiated PVC films.

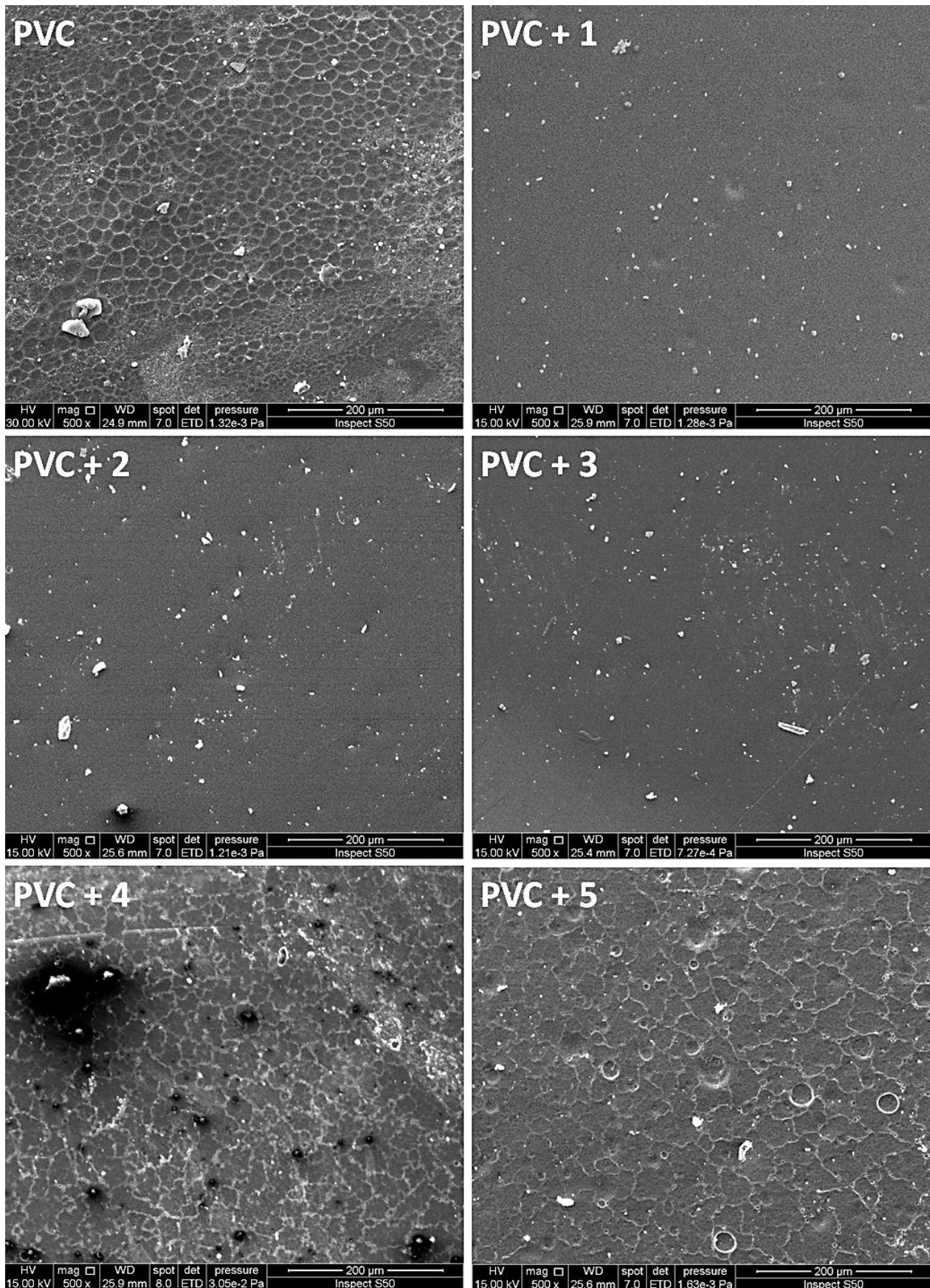


Figure 10. SEM images of the irradiated PVC films.

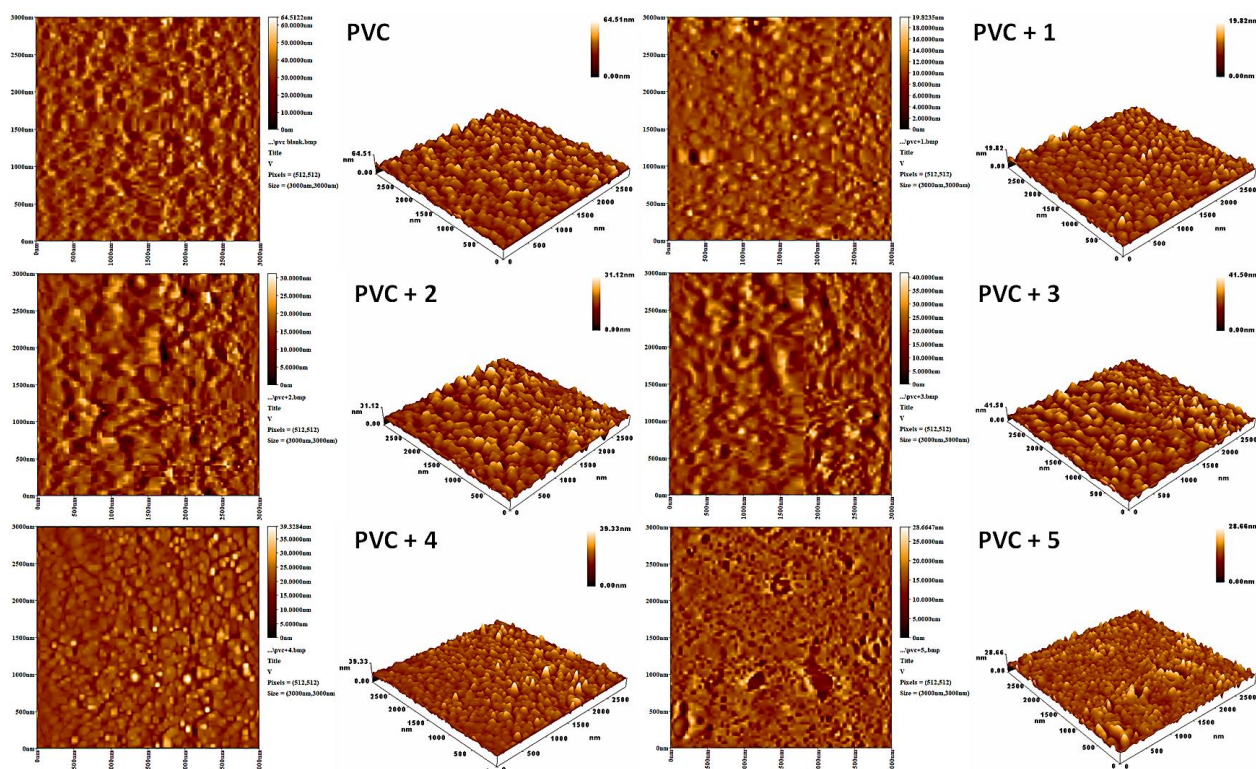
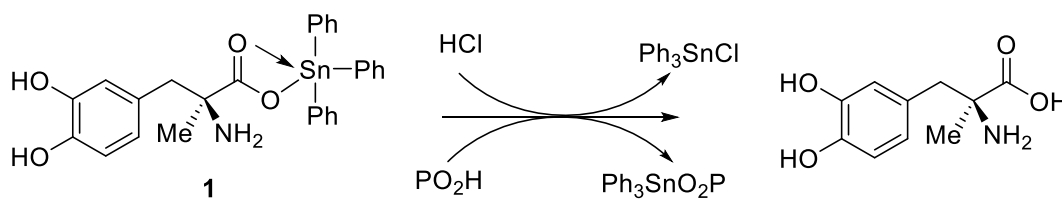


Figure 11. AFM images of the irradiated PVC films.

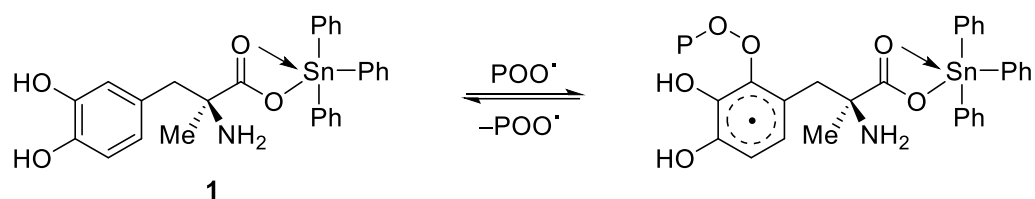
### 3.7. Suggested Mechanisms for Photostabilization

Methyldopa–tin complexes act as good PVC photostabilizers and reduce the damage due to photodegradation. The additives act as absorbers of harmful UV light, thereby protecting the polymer [73]. In addition, these stabilizers deactivate reactive species produced during photodegradation [74]. For example, the tin atom (a Lewis acid) in complex 1 can act as an acidic center and is, therefore, capable of scavenging the HCl (i.e., a secondary photostabilizer) released during photodegradation (Scheme 3). Moreover, the additives (e.g., complex 1) act as decomposers for the hydroperoxides ( $\text{PO}_2\text{H}$ ; Scheme 3) produced by the photodegradation of PVC [75].



Scheme 3. Complex 1 acts as an HCl and  $\text{PO}_2\text{H}$  decomposer.

The reactive species (e.g., peroxide radicals,  $\text{POO}^\bullet$ ) produced during PVC photodegradation can form stable intermediates with methyldopa–tin complexes (e.g., complex 1) as a result of the resonance within the aryl ring [76]. Thus complex 1 acts as a radical scavenger and leads to a significant stabilization of the PVC (Scheme 4).



**Scheme 4.** The function of complex **1** as a radical scavenger.

Finally, the interaction between the polarized atoms within the PVC (i.e., C–Cl bonds) and the heteroatoms (oxygen and nitrogen) within the organic motif in complexes could stabilize the polymer (Figure 12). However, in large molecules, such as blended PVC, steric hindrance may interfere with the effectiveness of the process.

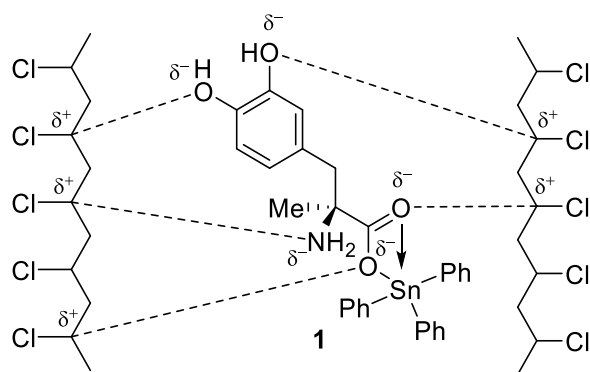


**Figure 12.** Coordination between PVC and complex **1** through polarized bonds.

#### 4. Conclusions

A simple procedure has been used to obtain, in high yield, five methyl dopa–tin complexes containing aromatic and aliphatic substituents. Polyvinyl chloride thin films can be damaged by ultraviolet irradiation, and the complexes have been assessed as additives for stabilization against irradiation. The use of a small concentration of methyl dopa–tin complexes as additives significantly improved the photostability of polyvinyl chloride. The methyl dopa–tin complexes coordinate well with the polymeric chains and act by absorbing the radiation. In addition, they act as radical, peroxide, and hydrogen chloride scavengers. The most effective additives were the ones containing aromatic residues. The methyl dopa–tin complexes clearly have the potential for application as stabilizers for polyvinyl chloride, but additional research is required to evaluate any health risks associated with these additives.

**Author Contributions:** Conceptualization: E.Y., D.S.A. and G.A.E.-H.; methodology: E.Y., D.S.A. and G.A.E.-H.; software: N.N., E.Y., D.S.A., B.M.K. and G.A.E.-H.; validation: N.N., E.Y., D.S.A., B.M.K. and G.A.E.-H.; formal analysis: E.Y., D.S.A. and G.A.E.-H.; investigation: N.N.; resources: E.Y., D.S.A. and G.A.E.-H.; data curation: N.N., E.Y., D.S.A. and G.A.E.-H.; writing—original draft preparation: E.Y., D.S.A., B.M.K. and G.A.E.-H.; writing—review and editing: E.Y., D.S.A., B.M.K. and G.A.E.-H.; project administration: E.Y.; funding acquisition: G.A.E.-H. All authors have read and agreed to the published version of the manuscript.

**Funding:** The research was supported by the Researchers Supporting Project (number RSP-2021/404), King Saud University, Riyadh, Saudi Arabia.

**Institutional Review Board Statement:** Not applicable.

**Informed Consent Statement:** Not applicable.

**Data Availability Statement:** Data are contained within the article.

**Acknowledgments:** We thank Al-Nahrain University for technical support. We acknowledge the support received from the Researchers Supporting Project (number RSP-2021/404), King Saud University, Riyadh, Saudi Arabia.

**Conflicts of Interest:** The authors declare no conflict of interest. The funders had no role in the design of the study, in the collection, analyses, or interpretation of data, in the writing of the manuscript, or in the decision to publish the results.

## References

1. Geyer, R.; Jambeck, J.R.; Law, K.L. Production, use, and fate of all plastics ever made. *Sci. Adv.* **2017**, *3*, e1700782. [[CrossRef](#)] [[PubMed](#)]
2. Zhang, Y.; Yu, X.; Cheng, Z. Research on the application of synthetic polymer materials in contemporary public art. *Polymers* **2022**, *14*, 1208. [[CrossRef](#)] [[PubMed](#)]
3. Young, R.J.; Lovell, P.A. *Introduction to Polymers*, 3rd ed.; CRC Press: Boca Raton, FL, USA, 2011; p. 76. [[CrossRef](#)]
4. Neuba, L.D.M.; Junio, R.F.P.; Ribeiro, M.P.; Souza, A.T.; Lima, E.D.S.; Filho, F.D.C.G.; Figueiredo, A.B.-H.D.S.; Braga, F.D.O.; De Azevedo, A.R.G.; Monteiro, S.N. Promising mechanical, thermal, and ballistic properties of novel epoxy composites reinforced with *Cyperus malaccensis* sedge fiber. *Polymers* **2020**, *12*, 1776. [[CrossRef](#)] [[PubMed](#)]
5. El-Hiti, G.A.; Ahmed, D.S.; Yousif, E.; Al-Khazrajy, O.S.A.; Abdallah, M.; Alanazi, S.A. Modifications of polymers through the addition of ultraviolet absorbers to reduce the aging effect of accelerated and natural irradiation. *Polymers* **2022**, *14*, 20. [[CrossRef](#)] [[PubMed](#)]
6. Chamas, A.; Moon, H.; Zheng, J.; Qiu, Y.; Tabassum, T.; Jang, J.H.; Abu-Omar, M.; Scott, S.L.; Suh, S. Degradation rates of plastics in the environment. *ACS Sustain. Chem. Eng.* **2020**, *8*, 3494–3511. [[CrossRef](#)]
7. Yaqoob, A.A.; Noor, N.H.M.; Serrà, A.; Mohamad Ibrahim, M.N. Advances and challenges in developing efficient graphene oxide-based ZnO photocatalysts for dye photo-oxidation. *Nanomaterials* **2020**, *10*, 932. [[CrossRef](#)]
8. Andrady, A.L.; Neal, M.A. Applications and societal benefits of plastics. *Philos. Trans. R. Soc. Lond. B Biol. Sci.* **2009**, *364*, 1977–1984. [[CrossRef](#)]
9. Lieberzeit, P.; Bekchanov, D.; Mukhamediev, M. Polyvinyl chloride modifications, properties, and applications: Review. *Polym. Adv. Technol.* **2022**, *33*, 1809–1820. [[CrossRef](#)]
10. Keane, M.A. Catalytic conversion of waste plastics: Focus on waste PVC. *J. Chem. Technol. Biotechnol.* **2007**, *82*, 787–795. [[CrossRef](#)]
11. Ma, Y.-F.; Liao, S.-L.; Li, Q.-G.; Guan, Q.; Jia, P.-Y.; Zhou, Y.-H. Physical and chemical modifications of poly(vinyl chloride) materials to prevent plasticizer migration—Still on the run. *React. Funct. Polym.* **2019**, *147*, 104458. [[CrossRef](#)]
12. Starnes, W.H., Jr. Structural and mechanistic aspects of the thermal degradation of poly(vinyl chloride). *Prog. Polym. Sci.* **2002**, *27*, 2133–2170. [[CrossRef](#)]
13. Lu, T.; Solis-Ramos, E.; Yi, Y.B.; Kumosa, M. Particle removal mechanisms in synergistic aging of polymers and glass reinforced polymer composites under combined UV and water. *Compos. Sci. Technol.* **2017**, *153*, 273–281. [[CrossRef](#)]
14. Lewandowski, K.; Skórczewska, K. A Brief review of poly(Vinyl chloride) (PVC) recycling. *Polymers* **2022**, *14*, 3035. [[CrossRef](#)] [[PubMed](#)]
15. Zhang, Q.; Wen, S.; Feng, Q.; Wang, H. Enhanced sulfidization of azurite surfaces by ammonium phosphate and its effect on flotation. *Int. J. Miner. Metall. Mater.* **2022**, *29*, 1150–1160. [[CrossRef](#)]
16. Zhao, W.; Wang, M.; Yang, B.; Feng, Q.; Liu, D. Enhanced sulfidization flotation mechanism of smithsonite in the synergistic activation system of copper–ammonium species. *Miner. Eng.* **2022**, *187*, 107796. [[CrossRef](#)]
17. Yu, J.; Sun, L.; Ma, C.; Qiao, Y.; Yao, H. Thermal degradation of PVC: A review. *Waste Manag.* **2016**, *48*, 300–314. [[CrossRef](#)]
18. Lu, T.; Solis-Ramos, E.; Yi, Y.; Kumosa, M. UV degradation model for polymers and polymer matrix composites. *Polym. Degrad. Stab.* **2018**, *154*, 203–210. [[CrossRef](#)]
19. Liu, J.; Lv, Y.; Luo, Z.; Wang, H.; Wei, Z. Molecular chain model construction, thermo-stability, and thermo-oxidative degradation mechanism of poly(vinyl chloride). *RSC Adv.* **2016**, *6*, 31898–31905. [[CrossRef](#)]
20. Folarin, O.M.; Sadiku, E.R. Thermal stabilizers for poly(vinyl chloride): A review. *Int. J. Phys. Sci.* **2011**, *6*, 4323–4330. [[CrossRef](#)]
21. Zheng, X.-G.; Tang, L.-H.; Zhang, N.; Gao, Q.-H.; Zhang, C.-F.; Zhu, Z.-B. Dehydrochlorination of PVC materials at high temperature. *Energy Fuels* **2003**, *17*, 896–900. [[CrossRef](#)]
22. Valko, L.; Klein, E.; Kovařík, P.; Bleha, T.; Šimon, P. Kinetic study of thermal dehydrochlorination of poly(vinyl chloride) in the presence of oxygen: III. Statistical thermodynamic interpretation of the oxygen catalytic activity. *Eur. Polym. J.* **2001**, *37*, 1123–1132. [[CrossRef](#)]
23. Gao, A.X.; Bolt, J.D.; Feng, A.A. Role of titanium dioxide pigments in outdoor weathering of rigid PVC. *Plast. Rubber Compos.* **2008**, *37*, 397–402. [[CrossRef](#)]
24. Chai, R.D.; Zhang, J. Synergistic effect of hindered amine light stabilizers/ultraviolet absorbers on the polyvinyl chloride/powder nitrile rubber blends during photodegradation. *Polym. Eng. Sci.* **2013**, *53*, 1760–1769. [[CrossRef](#)]
25. Cadogan, D.F.; Howick, C.J. Plasticizers. In *Ullmann's Encyclopedia of Industrial Chemistry*; Wiley-VCH: Weinheim, Germany, 2000.
26. Braun, D. Recycling of PVC. *Prog. Polym. Sci.* **2002**, *27*, 2171–2195. [[CrossRef](#)]

27. Porta, M.; Zumeta, E. Implementing the Stockholm treaty on persistent organic pollutants. *Occup. Environ. Med.* **2002**, *59*, 651–652. [[CrossRef](#)] [[PubMed](#)]
28. Grossman, R.F. Mixed metal vinyl stabilizer synergism. II: Reactions with zinc replacing cadmium. *J. Vinyl Addit. Technol.* **1990**, *12*, 142–145. [[CrossRef](#)]
29. Li, D.; Xie, L.; Fu, M.; Zhang, J.; Indrawirawan, S.; Zhang, Y.; Tang, S. Synergistic effects of lanthanum-pentaerythritol alkoxide with zinc stearates and with beta-diketone on the thermal stability of poly(vinyl chloride). *Polym. Degrad. Stab.* **2015**, *114*, 52–59. [[CrossRef](#)]
30. Fu, M.; Li, D.; Liu, H.; Ai, H.; Zhang, Y.; Zhang, L. Synergistic effects of zinc-mannitol alkoxide with calcium/zinc stearates and with  $\beta$ -diketone on thermal stability of rigid poly(vinyl chloride). *J. Polym. Res.* **2016**, *23*, 13. [[CrossRef](#)]
31. El-Hiti, G.A.; Ahmed, D.S.; Yousif, E.; Alotaibi, M.H.; Star, H.A.; Ahmed, A.A. Influence of polyphosphates on the physicochemical properties of poly(vinyl chloride) after irradiation with ultraviolet light. *Polymers* **2020**, *12*, 193. [[CrossRef](#)]
32. Schiller, M. *PVC Additives: Performance, Chemistry, Developments, and Sustainability*; Carl Hanser Verlag: Munich, Germany, 2015.
33. Yang, T.C.; Noguchi, T.; Isshiki, M.; Wu, J.H. Effect of titanium dioxide particles on the surface morphology and the mechanical properties of PVC composites during QUV accelerated weathering. *Polym. Compos.* **2016**, *37*, 3391–3397. [[CrossRef](#)]
34. Sabaa, M.W.; Oraby, E.H.; Abdel Naby, A.S.; Mohammed, R.R. Anthraquinone derivatives as organic stabilizers for rigid poly(vinyl chloride) against photo-degradation. *Eur. Polym. J.* **2005**, *41*, 2530–2543. [[CrossRef](#)]
35. Yang, T.C.; Noguchi, T.; Isshiki, M.; Wu, J.H. Effect of titanium dioxide on chemical and molecular changes in PVC sidings during QUV accelerated weathering. *Polym. Degrad. Stab.* **2014**, *104*, 33–39. [[CrossRef](#)]
36. Annuar, S.N.S.; Kamaludin, N.F.; Awang, N.; Chan, K.M. Cellular basis of organotin(IV) derivatives as anticancer metallodrugs: A review. *Front. Chem.* **2021**, *9*, 657599. [[CrossRef](#)] [[PubMed](#)]
37. Adeyemi, J.O.; Onwudiwe, D.C. Organotin(IV) dithiocarbamate complexes: Chemistry and biological activity. *Molecules* **2018**, *23*, 2571. [[CrossRef](#)] [[PubMed](#)]
38. Khan, N.; Farina, Y.; Mun, L.K.; Rajab, N.F.; Awang, N. Syntheses, characterization, X-ray diffraction studies and in vitro antitumor activities of diorganotin(IV) derivatives of bis(*p*-substituted-*N*-methylbenzylaminedithiocarbamates). *Polyhedron* **2015**, *85*, 754–760. [[CrossRef](#)]
39. Niu, L.; Li, Y.; Li, Q. Medicinal properties of organotin compounds and their limitations caused by toxicity. *Inorg. Chim. Acta* **2014**, *423*, 2–13. [[CrossRef](#)]
40. Pellerito, C.; Nagy, L.; Pellerito, L.; Szorcik, A. Biological activity studies on organotin (IV)<sup>n+</sup> complexes and parent compounds. *J. Organomet. Chem.* **2006**, *691*, 1733–1747. [[CrossRef](#)]
41. Davies, A.G. *Organotin Chemistry*, 2nd ed.; Wiley-VCH: Weinheim, Germany; John Wiley: Chichester, UK, 2004.
42. Mah, G.T.; Tejani, A.M.; Musini, V.M. Methyl dopa for primary hypertension. *Cochrane Database Syst Rev.* **2009**, *2009*, CD003893. [[CrossRef](#)]
43. Gardette, J.L.; Gaumet, S.; Lemaire, J. Photooxidation of poly(vinyl chloride). 1. A reexamination of the mechanism. *Macromolecules* **1989**, *22*, 2576–2581. [[CrossRef](#)]
44. Chaochanchaikul, K.; Rosarpitak, V.; Sombatsompop, N. Photodegradation profiles of PVC compound and wood/PVC composites under UV weathering. *Express Polym. Lett.* **2013**, *7*, 146–160. [[CrossRef](#)]
45. Pi, H.; Xiong, Y.; Guo, S. The kinetic studies of elimination of HCl during thermal decomposition of PVC in the presence of transition metal oxides. *Polym. Plast. Technol. Eng.* **2005**, *44*, 275–288. [[CrossRef](#)]
46. Gaumet, S.; Gardette, J.-L. Photo-oxidation of poly(vinyl chloride): Part 2—A comparative study of the carbonylated products in photo-chemical and thermal oxidations. *Polym. Degrad. Stab.* **1991**, *33*, 17–34. [[CrossRef](#)]
47. Pospíšil, J.; Nešpúrek, S. Photostabilization of coatings. Mechanisms and performance. *Prog. Polym. Sci.* **2000**, *25*, 1261–1335. [[CrossRef](#)]
48. Pepperl, G. Molecular weight distribution of commercial PVC. *J. Vinyl Addit. Technol.* **2000**, *6*, 88–92. [[CrossRef](#)]
49. Alcock, N.W.; Culver, J.; Roe, S.M. Secondary bonding. Part 15. Influence of lone pairs on coordination: Comparison of diphenyl-tin (IV) and -tellurium (IV) carboxylates and dithiocarbamates. *J. Chem. Soc. Dalton Trans.* **1992**, *9*, 1477–1484. [[CrossRef](#)]
50. Barroso-Flores, J.; Cea-Olivares, R.; Toscano, R.A.; Cogordan, J.A. Synthesis of the anisobidentate compound bis(2-amino-cyclopent-1-ene-carbodithioate)diethyltin (IV). Experimental and theoretical study. *J. Organomet. Chem.* **2004**, *689*, 2096–2102. [[CrossRef](#)]
51. Dragnevski, K.I.; Donald, A.M.; Clarke, S.M.; Maltby, A. Novel applications of ESEM and EDX for the study of molecularly thin amide monolayers on polymer films. *Colloid. Surf. A* **2009**, *337*, 47–51. [[CrossRef](#)]
52. Abd Mutalib, M.; Rahman, M.A.; Othman, M.H.D.; Ismail, A.F.; Jaafar, J. Scanning electron microscopy (SEM) and energy-dispersive X-Ray (EDX) spectroscopy. In *Membrane Characterization*; Hilal, N., Ismail, A.F., Matsuura, T., Oatley-Radcliffe, D., Eds.; Elsevier: Oxford, UK, 2017; Volume Chapter 9, pp. 161–179. [[CrossRef](#)]
53. Wang, Z.-M.; Wagner, J.; Ghosal, S.; Bedi, G.; Wall, S. SEM/EDS and optical microscopy analyses of microplastics in ocean trawl and fish guts. *Sci. Total Environ.* **2017**, *603–604*, 616–626. [[CrossRef](#)]
54. Karayıldırım, T.; Yanık, J.; Yüksel, M.; Sağlam, M.; Haussmann, M. Degradation of PVC containing mixtures in the presence of HCl fixators. *J. Polym. Environ.* **2005**, *13*, 365–379. [[CrossRef](#)]
55. Nief, O.A. Photostabilization of polyvinyl chloride by some new thiazazole derivatives. *Eur. J. Chem.* **2015**, *6*, 242–247. [[CrossRef](#)]



56. Jafari, A.J.; Donaldson, J.D. Determination of HCl and VOC emission from thermal degradation of PVC in the absence and presence of copper, copper(II) oxide and copper(II) chloride. *J. Chem.* **2009**, *6*, 685–692. [[CrossRef](#)]
57. Skillicorn, D.E.; Perkins, G.G.A.; Slark, A.; Dawkins, J.V. Molecular weight and solution viscosity characterization of PVC. *J. Vinyl Addit. Technol.* **1993**, *15*, 105–108. [[CrossRef](#)]
58. See, C.H.; O'Haver, J. Atomic force microscopy characterization of ultrathin polystyrene films formed by admicellar polymerization on silica disks. *J. Appl. Polym. Sci.* **2003**, *89*, 36–46. [[CrossRef](#)]
59. Nikafshar, S.; Zabihi, O.; Ahmadi, M.; Mirmohseni, A.; Taseidifar, M.; Naebe, M. The effects of UV light on the chemical and mechanical properties of a transparent epoxy-diamine system in the presence of an organic UV absorber. *Materials* **2017**, *10*, 180. [[CrossRef](#)] [[PubMed](#)]
60. Mehmood, N.; Andreasson, E.; Kao-Walter, S. SEM observations of a metal foil laminated with a polymer film. *Procedia Mater. Sci.* **2014**, *3*, 1435–1440. [[CrossRef](#)]
61. Kayyrapu, B.; Kumar, M.Y.; Mohommad, H.B.; Neeruganti, G.O.; Chekuri, R. Structural, thermal and optical properties of pure and Mn<sup>2+</sup> doped poly(vinyl chloride) films. *Mater. Res.* **2016**, *19*, 1167–1175. [[CrossRef](#)]
62. Hadi, A.G.; Yousif, E.; El-Hiti, G.A.; Ahmed, D.S.; Jawad, K.; Alotaibi, M.H.; Hashim, H. Long-term effect of ultraviolet irradiation on poly(vinyl chloride) films containing naproxen diorganotin(IV) complexes. *Molecules* **2019**, *24*, 2396. [[CrossRef](#)]
63. Mousa, O.G.; El-Hiti, G.A.; Baashen, M.A.; Bufaroosha, M.; Ahmed, A.; Ahmed, A.A.; Ahmed, D.S.; Yousif, E. Synthesis of carvedilol-organotin complexes and their effects on reducing photodegradation of poly(vinyl chloride). *Polymers* **2021**, *13*, 500. [[CrossRef](#)]
64. Ali, M.M.; El-Hiti, G.A.; Yousif, E. Photostabilizing efficiency of poly(vinyl chloride) in the presence of organotin(IV) complexes as photostabilizers. *Molecules* **2016**, *21*, 1151. [[CrossRef](#)]
65. Mohammed, A.; El-Hiti, G.A.; Yousif, E.; Ahmed, A.A.; Ahmed, D.S.; Alotaibi, M.H. Protection of poly(vinyl chloride) films against photodegradation using various valsartan tin complexes. *Polymers* **2020**, *12*, 969. [[CrossRef](#)]
66. Hadi, A.G.; Jawad, K.; El-Hiti, G.A.; Alotaibi, M.H.; Ahmed, A.A.; Ahmed, D.S.; Yousif, E. Photostabilization of poly(vinyl chloride) by organotin(IV) compounds against photodegradation. *Molecules* **2019**, *24*, 3557. [[CrossRef](#)] [[PubMed](#)]
67. Yaseen, A.A.; Yousif, E.; Al-Tikrity, E.T.B.; El-Hiti, G.A.; Kariuki, B.M.; Ahmed, D.S.; Bufaroosha, M. FTIR, weight, and surface morphology of poly(vinyl chloride) doped with tin complexes containing aromatic and heterocyclic moieties. *Polymers* **2021**, *13*, 3264. [[CrossRef](#)] [[PubMed](#)]
68. Fadhil, M.; Yousif, E.; Ahmed, D.S.; Mohammed, A.; Hashim, H.; Ahmed, A.; Kariuki, B.M.; El-Hiti, G.A. Synthesis of new norfloxacin–tin complexes to mitigate the effect of ultraviolet-visible irradiation in polyvinyl chloride films. *Polymers* **2022**, *14*, 2812. [[CrossRef](#)] [[PubMed](#)]
69. Fadhil, M.; Yousif, E.; Ahmed, D.S.; Kariuki, B.M.; El-Hiti, G.A. Synthesis and application of levofloxacin–tin complexes as new photostabilizers for polyvinyl chloride. *Polymers* **2022**, *14*, 3720. [[CrossRef](#)] [[PubMed](#)]
70. Ghazi, D.; El-Hiti, G.A.; Yousif, E.; Ahmed, D.S.; Alotaibi, M.H. The effect of ultraviolet irradiation on the physicochemical properties of poly(vinyl chloride) films containing organotin(IV) complexes as photostabilizers. *Molecules* **2018**, *23*, 254. [[CrossRef](#)]
71. Ghani, H.; Yousif, E.; Ahmed, D.S.; Kariuki, B.M.; El-Hiti, G.A. Tin complexes of 4-(benzylideneamino)benzenesulfonamide: Synthesis, structure elucidation and their efficiency as PVC photostabilizers. *Polymers* **2021**, *13*, 2434. [[CrossRef](#)]
72. Hadi, A.G.; Baqir, S.J.; Ahmed, D.S.; El-Hiti, G.A.; Hashim, H.; Ahmed, A.; Kariuki, B.M.; Yousif, E. Substituted organotin complexes of 4-methoxybenzoic acid for reduction of poly(vinyl chloride) photodegradation. *Polymers* **2021**, *13*, 3946. [[CrossRef](#)]
73. Larché, J.F.; Bussière, P.O.; Therias, S.; Gardette, J.L. Photooxidation of polymers: Relating material properties to chemical changes. *Polym. Degrad. Stab.* **2012**, *97*, 25–34. [[CrossRef](#)]
74. Scott, G. *Mechanism of Polymer Degradation and Stabilization*; Elsevier: New York, NY, USA, 1990.
75. Pospíšil, J.; Klemchuk, P.P. *Oxidation Inhibition in Organic Materials*; CRC Press: Boca Raton, FL, USA, 1989; Volume 1, pp. 48–49.
76. Sabaa, M.W.; Oraby, E.H.; Abdel Naby, A.S.; Mohamed, R.R. N-phenyl-3-substituted 5-pyrazolone derivatives as organic stabilizers for rigid poly (vinyl chloride) against photodegradation. *J. Appl. Polym. Sci.* **2006**, *101*, 1543–1555. [[CrossRef](#)]